Pol. J. Environ. Stud. Vol. XX, No. X (XXXX), 1-11
DOI: *10.15244/pjoes/217137* ONLINE PUBLICATION DATE: 2026-03-04

Original Research

Analysis of Microbial Community Structure and Dynamic Changes during the Domestication Process of Embedded Particles

Linxue Zheng[1, 2], Fuping Li[1, 2]*, Hao Wang[1, 2], Yanjun Ai[1, 2], Yijun Zhou[3]

[1]College of Mining Engineering, North China University of Science and Technology, Tangshan 063210, China
[2]Hebei Industrial Technology Institute of Mine Ecological Remediation, Tangshan 063210, China
[3]College of Civil and Architectural Engineering, North China University of Science and Technology, Tangshan 063210, China

Received: 20 October 2025
Accepted: 19 January 2026

Abstract

The nitrification process is highly feasible for treating high-ammonia nitrogen and low C/N ratio wastewater. By using thermal shock to treat embedded activated sludge, the accumulation of NO_2^--N has been successfully achieved. To study the changes in microbial communities within the embedded particles before and after heat shock, and to reveal their succession patterns and dominant flora, the present experiment was carried out to analyze the community structure of microorganisms in the three phases of pre-domestication, post-domestication, and post-heat-shock by using Polymerase Chain Reaction-Denaturing Gradient Gel Electrophoresis (PCR-DGGE), as well as to carry out species identification and phylogenetic analyses by the molecular cloning method. The 16S rDNA sequence analysis of the characteristic bands of the total bacterial DGGE spectrum showed that the activated sludge had the most species before domestication. As domestication proceeded, the total bacterial diversity decreased. In contrast, the species of ammonia-oxidizing bacteria (AOB) and nitrite-oxidizing bacteria (NOB) increased significantly, and the nitrification performance of the sludge was enhanced. The thermal shock did not have a significant effect on the diversity of the AOB populations but had a great effect on the NOBs, and the dominant genera of the NOBs were almost completely inactivated.

Keywords: nitrosation, embedded particles, PCR-DGGE, microbial community structure

Introduction

Short-cut nitrification is the process of controlling the conversion of ammonia nitrogen to nitrite nitrogen by taking advantage of the differences between AOB and NOB under different conditions, so that AOB are in the dominant strain in the system [1, 2]. Compared with the traditional full nitrification process, short-cut nitrification has gradually become an indispensable part of many new nitrogen removal processes due to its ability to effectively reduce the energy demand during wastewater treatment, reduce organic carbon

*e-mail: lifuping@ncst.edu.cn

consumption, and reduce sludge production [3-5]. However, it is difficult to control the nitrification process completely at the nitrite stage, and the key is to control the ratio of AOB and NOB to achieve nitrite accumulation [6, 7].

Heat treatment is one of the most effective means to inhibit NOB in recent years, taking advantage of the difference in temperature sensitivity between AOB and NOB to rapidly phase out NOB [8, 9]. It was shown that the optimum growth temperature of AOB was 25-30ºC, while NOB was more active at 10-20ºC [10]. When the temperature was higher than 30ºC, the specific growth rate of AOB was greater than that of NOB, thus NO_2^--N accumulation occurred in the reactor [11, 12]. Recent studies have further confirmed that short-term high-temperature thermal shock (e.g., 55-60ºC for several hours) can more persistently disrupt the community structure of nitrite-oxidizing bacteria (NOB), offering a novel strategy for rapidly initiating partial nitrification [13]. In addition to temperature control, other physical methods, such as ultrasound irradiation, can also optimize treatment effectiveness by altering microbial activity or substance transformation pathways [14]. This further demonstrates that selectively regulating microorganisms through external physicochemical means is an effective approach to achieving partial nitrification.

In recent years, embedding immobilization technology has been one of the research hotspots in the field of wastewater nitrogen removal. This technique encapsulates microorganisms within gel carriers (such as polyvinyl alcohol-sodium alginate, PVA-SA), creating a protective microenvironment [15, 16]. Its advantage lies in allowing small molecules such as substrates and oxygen to diffuse through the carrier pores, supplying microbial metabolism, while ensuring that metabolic products can effectively diffuse to the outside of the carrier [17, 18]. Studies have shown that using PVA-SA to embed partial nitrification activated sludge can achieve stable nitrite accumulation (with a nitrite accumulation rate exceeding 86%) in continuous-flow reactors, while significantly increasing the relative abundance of AOB (such as *Nitrosomonas*) within the embedded carriers [19]. Furthermore, optimizing operational parameters of the embedded fillers (such as dissolved oxygen, hydraulic retention time, and filling ratio) is crucial for achieving efficient partial nitrification-denitrification [20]. Similarly, cross-disciplinary research between materials science and environmental engineering also provides new perspectives for pollution control [21].

In this experiment, the activated sludge was used to make embedded bacterial particles, and a new way was adopted to achieve stable nitrification by "thermal shock" of the embedded particles at a certain temperature. Combined with PCR-DGGE technology and 16S rDNA homology comparative analysis, the changes in microbial communities in the embedded particles after thermal shock were investigated, revealing their succession patterns and dominant bacterial communities, in order to provide a theoretical basis for a new type of nitrification process based on embedding fixation. It is worth noting that the ultimate goal of efficient nitrogen removal processes, such as short-cut nitrification, is not only wastewater purification but also water resource recovery and reuse. For example, Mukheef et al. explored the use of treated wastewater for artificial recharge of unconfined aquifers as a strategy to address climate change [22]. This further highlights the potential value of this study in promoting the synergistic development of wastewater treatment and resource recovery.

Materials and Methods

Test Device and Sample Collection

Test Device

A 2 L plexiglass reactor was adopted in the continuous-flow experiments, as shown in Fig. 1. The upper part of the reactor was equipped with an overflow weir. The bottom was filled with water, and excess water overflowed from the upper part. The outlet was equipped with a grid to prevent embedded particles from flowing out with water. The reactor was equipped with an aeration device to fully aerate and maintain DO at above 4 mg/L. The reactor was equipped with a water bath on the outside, and the temperature inside the reactor was controlled to remain at 21ºC. The embedded bacteria for the test were 3×3×3 mm black cubes, which were prepared from polymer materials with good nitrification properties and mechanical stability.

Sample Collection

A continuous-flow experiment was adopted, and artificial water was used for water distribution. The main components are shown in Table 1, where NH_4^+-N and NO_2^--N are provided by NH_4Cl and $NaNO_2$, respectively. The NH_4^+-N concentration in the influent was maintained at 100 mg/L according to the experimental needs, and the effluent water quality was recorded daily. After thermal shock treatment at 60ºC for 10 min, the embedded particles were added to the reactor at a volume filling rate of 10%. At the same time, the embedded particles without heat shock treatment were used as the control group for testing. NH_4^+-N, NO_2^--N, and NO_3^--N indicators in the inlet and outlet water were sampled and measured at regular intervals every day, and the accumulation rate of NO_2^--N was calculated. The sludge was sampled three times, with the first sampling before domestication, the second sampling after domestication, and the third sampling after thermal shock (heating at 60ºC for 20 min). The sample numbers were labeled A, B, and C.

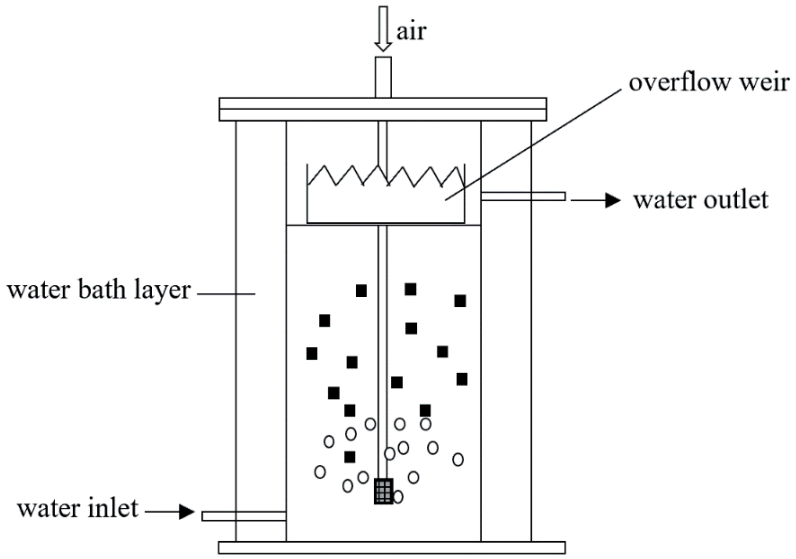

Fig. 1. The continuous tank reactor.

Test Methods

Water Quality Analysis Methods

NH_4^+-N: Nessler's reagent spectrophotometry; NO_2^--N: N-(1-naphthyl)-ethylenediamine spectrophotometric method; NO_3^--N: Thymol spectrophotometric method; pH/DO/Temperature: WTW/Multi3420 tester.

DNA Extraction

The sludge samples were sedimented in a 1.5 mL centrifuge tube for 10 min, and then the supernatant was removed. After high-speed centrifugation at 15,000 rpm for 5 min, the supernatant was removed. A 0.3 g sludge sample was taken for total DNA extraction, and the remaining sludge was frozen for later use. After extraction using the Ezup Column Genomic DNA Extraction Kit (Sangon Biotech), 5 μL of extract was taken and detected by 1.2% agarose gel. The rest was stored at -20ºC for later use.

Landing PCR Amplification of Total Bacteria

The DNA extracted in the previous step was used as the template, and the primers F341-GC (5'-CGCCCGCCGCGCCCCGCGCCCGTCCCGC CGCCCCCGCCCGCCTACGGGAGGCAGCAG -3') and EU500 (5'-GTATTACCGCGGCTGCTGG -3') with specificity for the V3 region of the 16S rDNA gene of most bacteria were used for PCR amplification. The PCR reaction system (50 μL) included 10×PCR buffer 5 μL, dNTP (each 2.5 $mmolL^{-1}$) 4 μL, F341-GC (20 $\mu molL^{-1}$) 1 μL, EU500 (20 $\mu molL^{-1}$) 1 μL, Taq DNA polymerase (5 U) 0.5 μL, DNA template 2 μL, and ddH_20 36.5 μL, and the final volume of the reaction was 50 μL. The PCR adopted the landing amplification procedure, and the specific reaction conditions were as follows: pre-denaturation at 94ºC for 5 min; denaturation at 94ºC for 1 min, annealing at 65ºC for 1 min, extension at 72ºC for 1 min, 20 cycles in total, each cycle reduced by 0.5ºC; denaturation at 94ºC for 1 min, annealing at 55ºC for 1 min, extension at 72ºC for 1 min, 3 cycles in total; extension at 72ºC for 10 min.

Nested PCR amplification of AOB

In order to enhance the sensitivity of PCR amplification and the specificity of DGGE analysis, nested PCR technology was used for AOB. Using primer pairs specific to AOB, the upstream primers were CTO189fA: 5'-GGAGAAAGCGGGATCG-3', CTO189fB: 5'-GGAGAAAGCAGGGGATCG-3', and CTO189fC: 5'-GGAGAAAGTAGGGATCG-3', with

Table 1. Artificial modeling of wastewater composition.

Main components	Mass concentration/($mg \cdot L^{-1}$)	Main components	Mass concentration/($mg \cdot L^{-1}$)
$NaHCO_3$	585	NH_4Cl	191
$CaCl_2$	11	$NaNO_2$	246
$MgSO_4 \cdot 7H_2O$	42	NaCl	25
$NaH_2PO_4 \cdot 12H_2O$	58	KCl	34

an equal molar mixture. The downstream primer was CTO654r: 5'-CTAGCYTTGTAGTTTCAAACGC-3', which merged with base Y (C, T). The first round of PCR used primers for specific target AOB and their corresponding PCR conditions. The second round of PCR used the product of the first round of PCR as a template and used primers F357-GC and R518 for amplification. The composition of the reaction system for the two rounds of PCR is shown in Table 2.

The procedure for the first round of reaction was as follows: pre-denaturation at 94ºC for 5 min; each cycle: denaturation at 94ºC for 45 s, annealing at 57ºC for 45 s, extension at 72ºC for 90 s, a total of 35 cycles; at the end of the cycle, extension at 72ºC for 10 min. The procedure for the second round of reaction was the same as that in subsection "DNA Extraction".

Nested PCR amplification of NOB

Similar to AOB, nested PCR technology was also used for NOB. The NOB-specific primer pairs were used; the upstream primer was FGPS1269: 5'-TTTTTGAGATTTGCTAG-3' and the downstream primer was FGPS872: 5'-CTAAAACTCAAAGGAATTGA-3'. The target-specific NOB primers and their corresponding PCR conditions were used in the first round of PCR. The product of the first round of PCR was used as a template in the second round of PCR using primers F357-GC and R518. The two rounds of PCR reaction systems were the same as those of AOB in subsection 1.2.3, except that the primers were different, as shown in Table 2.

The first round of reaction procedure was as follows: pre-denaturation at 94ºC for 3 min; amplification at 94ºC for 1 min, 50ºC for 1 min, 72ºC for 2 min for 30 cycles; and finally, extension at 72ºC for 3 min. The second round of reaction procedure was the same as that in subsection "DNA Extraction".

DGGE Gel Electrophoresis

The PCR amplification products were separated by the Bio-Rad DCode™ DGGE system. The gradient mixing device was used to prepare 8% polyacrylamide gels. The denaturation range of polypropylene gel was 35%-55% (100% of the denaturant was a mixture of 7 $mol \cdot L^{-1}$ urea and 40% formamide). The concentration of denaturant and acrylamide increased sequentially from the top to the bottom of the gel. After the polypropylene gel was completely solidified, the gel plate was put into an electrophoresis tank with electrophoresis buffer. The 20 μL of PCR samples and 10 μL of 6× loading buffer were mixed and added to the upper sample wells, and then electrophoresis was performed in 1× TAE electrophoresis buffer for 8 h (60ºC, 130 V). After electrophoresis, the gel was stained with Gel Red nucleic acid gel dye for 30 min and photographed in a gel imaging system (Gel Doc TMXR+, Bio-Rad).

Cloning and Sequencing

The main bands on the gel were cut using a sterilized knife, and they were placed in a 1.5 mL centrifuge tube. The 50 μL of sterilized deionized water was added to the tube. Then, the samples were placed at 4ºC overnight to allow the DNA fragments to slowly diffuse out of the gel, which was used as a template for PCR amplification using the F341 and EU500 primers without a GC-clamp structure. The amplification procedure was the same as in subsection "DNA Extraction". The PCR products were detected and purified by 1.2% agarose gel electrophoresis. The purified DNA fragment was connected to the PM18-T Vector (TaKaRa, Japan) and transformed into JM109 competent cells. Then, blue and white spots were screened on an LB plate containing X-gal, IPTG, and ampicillin (Amp). White spots were selected for colony PCR validation, and PCR products with the correct fragment size were sent to Shanghai Biotech for sequencing.

Results and Discussion

Analysis of Reactor Operation

From Fig. 2, it can be seen that the embedded particles exhibit good nitrification performance. On the first day, NH_4^+-N removal occurred, and the removal

Table 2. Nested PCR system of AOB.

Reagent	First round of PCR	Second round of PCR	Blank control
10×Buffer	5 μL	5 μL	5 μL
Forward Primer	0.5 μL	1 μL	1 μL
Reverse Primer	0.5 μL	1 μL	1 μL
dNTPs	4 μL	2 μL	2 μL
DNA template	1 μL	1 μL	-
Taq DNA polymerase	0.5 μL	0.5 μL	0.5 μL
Sterilized ultrapure water topped up to	50 μL	50 μL	50 μL

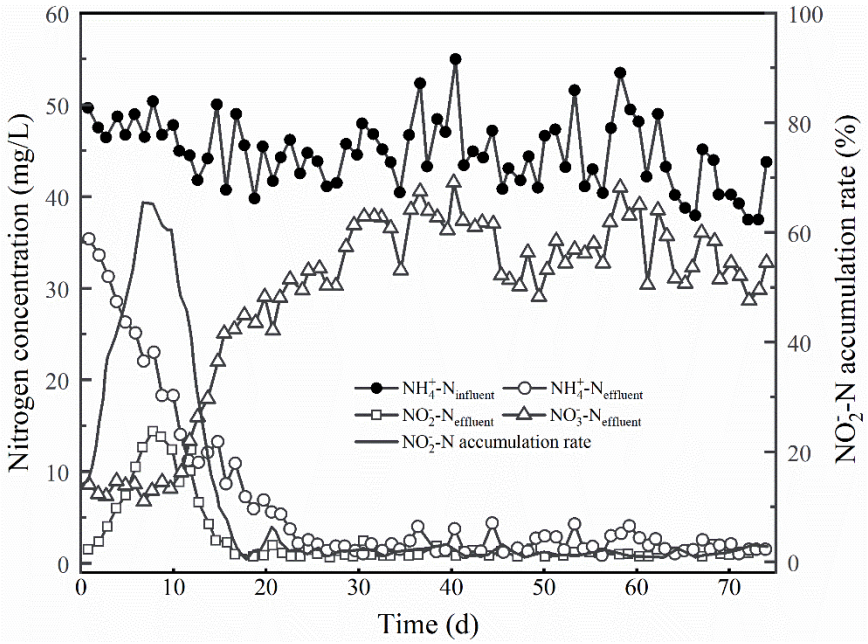

Fig. 2. The nitrogen removal characteristics of untreated embedded particles.

rate gradually increased. By the 26th day, the NH_4^+-N mass concentration in the effluent was 1.86 mg/L, and the ammonia nitrogen removal rate reached 95.7%. In the early stage of the experiment, untreated embedded particles also showed certain nitrosation performance. On the 7th day, the accumulation rate of NO_2^--N in the reactor reached 65.1%. This is mainly due to the presence of embedded materials, which can affect the mass transfer efficiency of oxygen, resulting in a lower oxygen concentration inside the embedded particles and causing the accumulation of NO_2^--N. Related research clearly indicates that this mass transfer limitation leads to nitrite accumulation [23]. As time goes on, the mass transfer efficiency of the embedded particles increases, and the nitrification performance gradually strengthens. After the embedded particles were subjected to 60ºC thermal shock treatment, as shown in Fig. 3, stable removal of NH_4^+-N began on the 12th day. The effluent NO_3^-- N was basically 0, and the NO_2^--N accumulation rate remained stable at over 90%. Compared with the embedded particles without thermal shock treatment, the embedded particles after thermal shock can reach

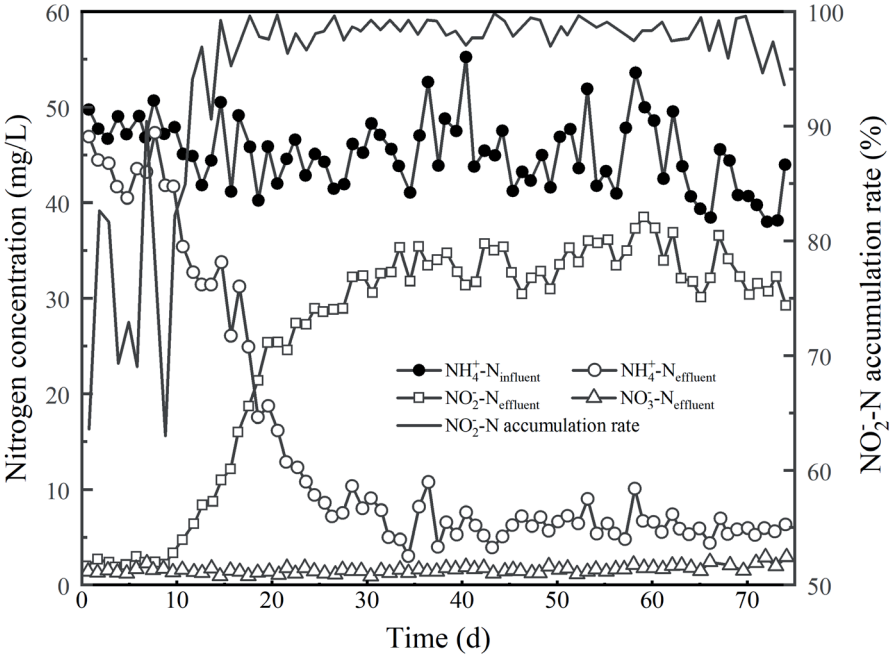

Fig. 3. The nitrogen removal characteristics of embedded particles subjected to 60°C thermal shock treatment.

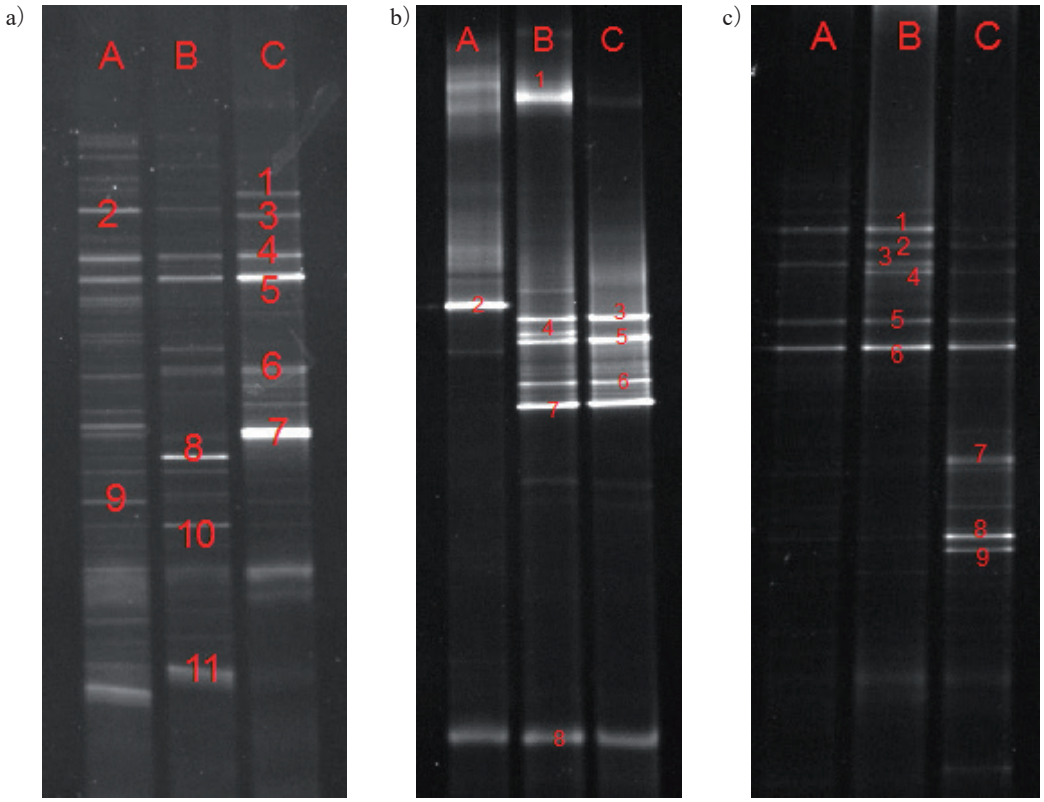

Fig. 4. PCR-DGGE profile in different phases. a) the total bacteria; b) AOB; c) NOB.

a NO_2^--N accumulation rate of over 90% and maintain stable operation. This is largely consistent with the findings of Li Xiang et al., who achieved stable partial nitrification in a continuous-flow AO reactor using PVA-SA-embedded shortcut nitrification activated sludge, with the system reaching a nitrite accumulation rate of 86.22% under optimal conditions [19].

DGGE Mapping Analysis

To investigate the changing pattern of community structure of total bacteria, AOB, and NOB in the three stages of pre-domestication, post-domestication, and post-heat-shock, the microorganisms in these three stages were analyzed by denaturing gradient gel electrophoresis (DGGE), respectively. The DGGE profiles of sludge samples at different stages are shown in Fig. 4, and the similarity of each lane is shown in Fig. 5.

From Figs 5 and 6 it can be concluded that the number of visible bands of total bacteria before domestication, after domestication, and after heat shock were 17, 13, and 10, respectively. The visible bands of AOB before domestication, after domestication, and after heat shock were 2, 7, and 5, respectively. The visible bands of NOB before domestication, after domestication, and after heat shock were 4, 6, and 5, respectively. From Fig. 4a), it can be seen that there were more types of activated sludge before domestication. Compared with before domestication, the number of bands decreased, and the brightness decreased after domestication, indicating a decrease in total bacterial species, a significant increase in the number of AOB and NOB species, and an enhancement of sludge nitrification performance. After heat shock, bands 1 and 4 in Fig. 4b) disappeared, while bands 3, 5, 6, 7, and 8 remained unchanged, indicating that heat shock had little effect on the diversity of AOB populations. In Fig. 4c), bands 1, 2, 3, and 4 basically disappeared, and almost all NOB dominant genera were inactivated, indicating that the biomass of NOB was reduced and the species decreased after the heat shock. At the same time, a number of new species adapted to the temperature environment were added, such as bands 7, 8, and 9.

Similarity Analysis in DGGE Mapping of Sludge Samples

Tables 3, 4, and 5 showed the similarity coefficients of total bacterial populations, AOB, and NOB between stages, respectively. The similarity coefficients between total bacterial samples A, B, and C were all low, roughly around 20-30%, indicating that the structure of microbial populations changed considerably before domestication, after domestication, and after heat shock. The similarity coefficients between AOB Sample A and Sample B, and Sample A and Sample C were only 3.9% and 3.8%, indicating that the community structure of AOB changed considerably with domestication. The similarity coefficient between Sample B and Sample C

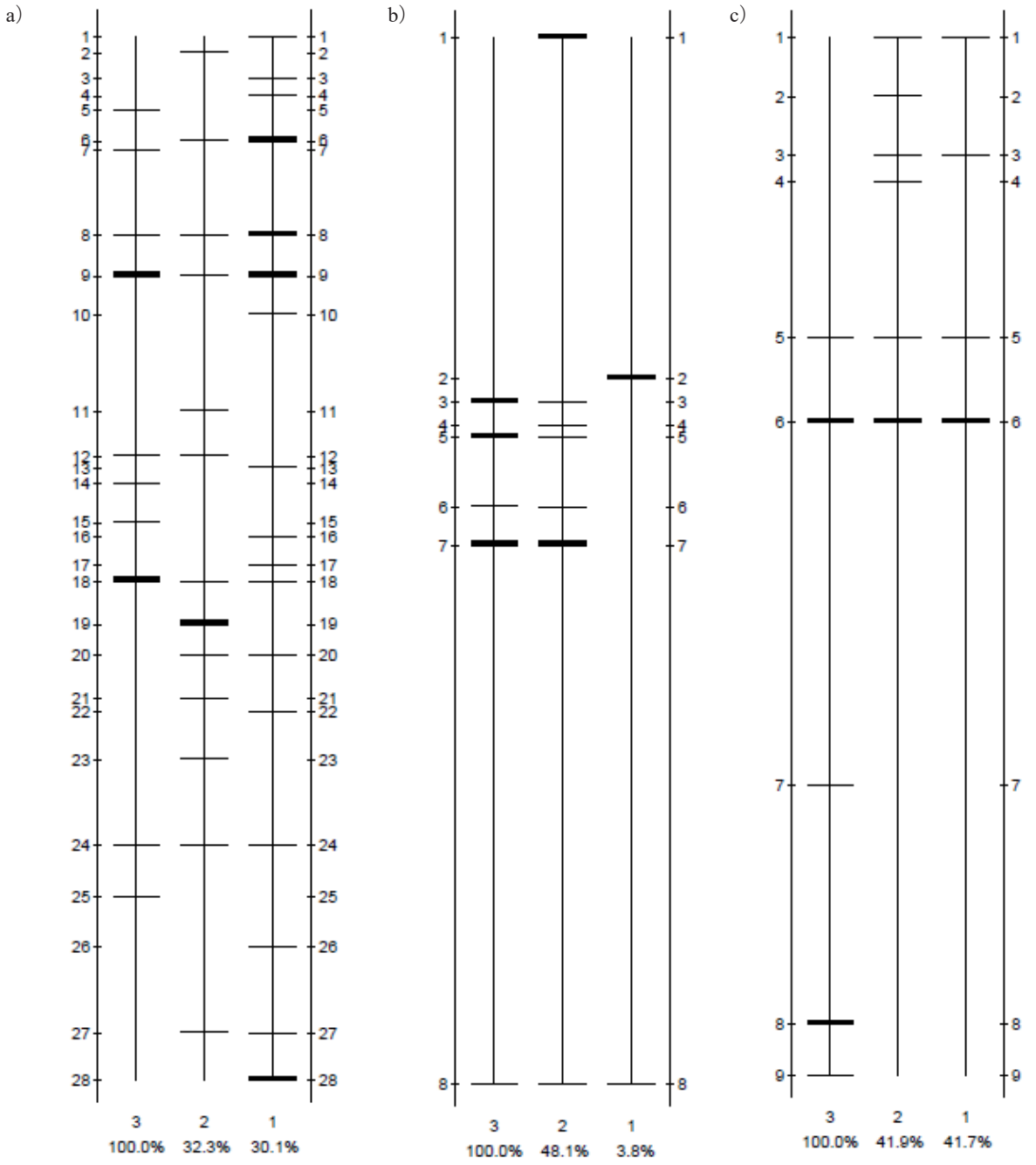

Fig. 5. Similarity comparison of DGGE bands. a) the total bacteria; b) AOB; c) NOB.

was relatively high (48.1%), indicating that heat shock had little effect on the diversity of AOB populations. The similarity coefficient between NOB sample A and sample B was 78.8%. The similarity coefficient between Sample B and Sample C was 41.9%, which is relatively low, again indicating that thermal shocks have a greater impact on the diversity of NOB populations.

Fragment Sequencing Analysis and Bacterial Species Identification of Total Bacteria

The PCR product of the DNA obtained from the DGGE profile of total bacteria in Fig. 4a) was sent to Shanghai Sangong Biotechnology Company for sequencing. One of the 11 DNA samples sent failed sequencing (sample T9), resulting in the acquisition of 10 16S rDNA sequences from the total bacteria. The gene sequences obtained from sequencing were entered into the NCBI website, and the sequences were compared and analyzed with the existing sequences in the database using the BLAST program. The main results of the comparison are shown in Table 6. At the same time, the evolutionary tree was constructed using the MEGA4 software, and the algorithm was neighbor-joining analysis, and the resulting evolutionary tree is shown in Fig. 6.

From Table 6, it can be seen that the similarity between the bacteria of the cloned library and the

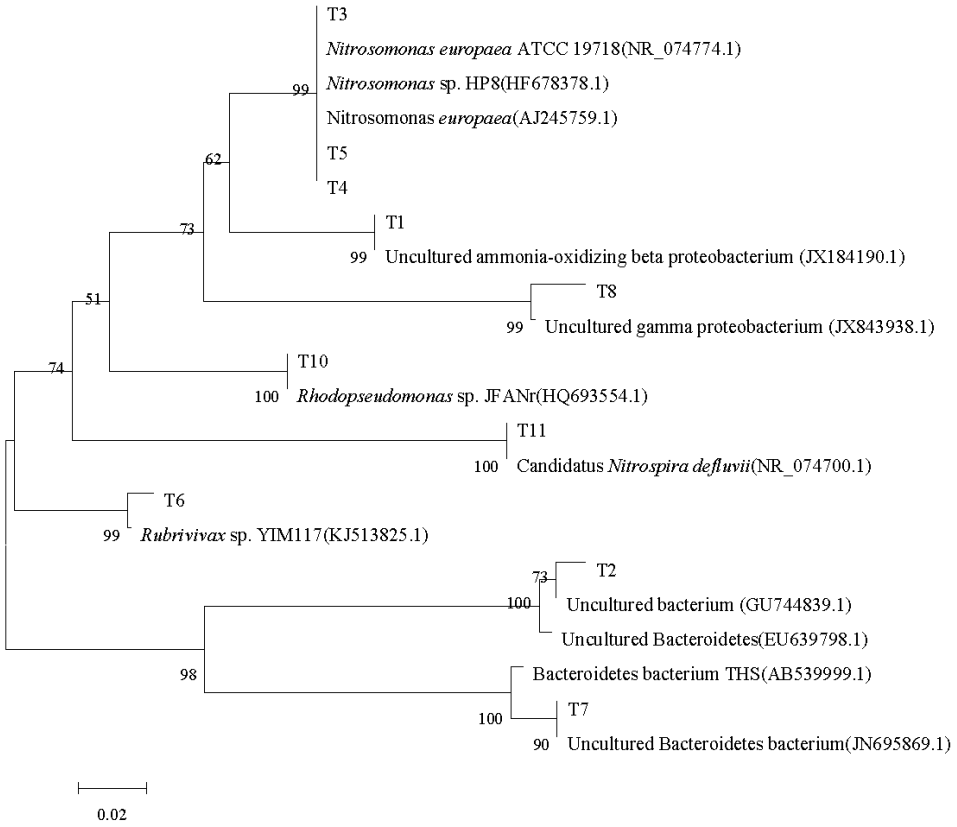

Fig. 6. A phylogenetic tree showing the total bacterial microbial community in sludge based on 16S rDNA sequences.

bacteria in the GenBank database ranges from 97% to 100%. The main dominant species present in sludge include β-Proteobacteria, γ-Proteobacteria, α-Proteobacteria, Nitrospira, and Uncultured. As shown in Fig. 6, bands T3, T4, and T5 were closely related to the genus *Nitrosomonas*, which belongs to the typical AOB microbial community. *Nitrosomonas*, as a dominant microbial community in short-range nitrification systems, has been reported in many r eports [24-28]. Band T11 was on the same branch as Nitrospira, a typical NOB bacterial group [29]. It was present only in the sample A and sample B environments and disappeared after heat shock. Band T1, which did not appear in the first two stages, was a new strain after heat shock. It had 99% similarity to an uncultured ammonia-oxidizing beta proteobacterium (JX184190.1), which was found in abandoned tin mine ponds in Pal, Perak. Band T2 showed 97% similarity to an uncultured bacterium (GU744839.1), which was detected using high-throughput sequencing in a drinking water treatment pilot-scale [30]. Band T6 was present in all three stages and showed 98% similarity to *Rubrivivax sp. YIM117* (KJ513825.1), which was found in the eutrophic waters of lakes. Band T7 was the dominant bacterial genus in sample C, with a 100% similarity to uncultured Bacteroidetes bacteria (JN695869.1), which was isolated in an MBR reactor. Bacteroidetes bacteria are frequently reported to be associated with polysaccharide degradation in many

Table 3. Comparability index of the total bacterial community from different samples (100%).

Sample	A	B	C
A	100	22.5	30.1
B	22.5	100	32.3
C	30.1	32.3	100

Table 4. Comparability index of the AOB bacterial community from different samples (100%).

Sample	A	B	C
A	100	3.9	3.8
B	3.9	100	48.1
C	3.8	48.1	100

Table 5. Comparability index of the NOB bacterial community from different samples (100%).

sample	A	B	C
A	100	78.8	41.7
B	78.8	100	41.9
C	41.7	41.9	100

Table 6. Similarity sequence of predominant DGGE band.

Band number	Length (bp)	Maximum similarity bacteria in GenBank	Login Number	Similarity (%)	Classification
T1	169	Uncultured ammonia-oxidizing beta proteobacterium	JX184190.1	99	*β*-Proteobacteria
T2	165	Uncultured bacterium	GU744839.1	97	Uncultured
T3	170	*Nitrosomonas* sp. Hp8	HF678378.1	98	*β*-Proteobacteria
T4	170	*Nitrosomonas europaea* atcc 19718	NR_074774.1	100	*β*-Proteobacteria
T5	168	Nitrosomonas europaea	AJ245759.1	99	*β*-Proteobacteria
T6	174	*Rubrivivax* sp. Yim117	KJ513825.1	98	*β*-Proteobacteria
T7	165	Uncultured bacteroidetes bacterium	JN695869.1	100	Bacteroidetes
T8	173	Uncultured gamma proteobacterium	JX843938.1	97	*γ*-Proteobacteria
T10	149	*Rhodopseudomonas* sp. Jfanr	HQ693554.1	99	*α*-Proteobacteria
T11	171	Candidatus *nitrospira defluvii*	NR_074700.1	99	*Nitrospira*

wastewater treatment systems and may play a significant role in the decomposition of organic matter[31]. Band T8 was the dominant bacterial genus after domestication, with a similarity of 97% to uncultured gamma proteobacteria (JX843938.1). This bacterium belonged to the γ-proteobacteria and was isolated in anaerobic sludge systems[32]. Band T10 was present in the first two phases and disappeared after thermal shock, with 99% similarity to *Rhodopseudomonas* sp. JFANr (HQ693554.1), which belonged to the α-Proteobacteria and was found in desulfurization reactors.

It is worth noting that out of the 10 bands successfully sequenced for total bacteria, only bands T1, T3, T4, and T5 were identified as AOB. However, DGGE detection of AOB using nested PCR resulted in 8 AOB bands, far exceeding the number of AOB bands in the total bacterial DGGE map. The reason for this phenomenon is that, firstly, due to the limitations of PCR-DGGE technology itself, it can only detect dominant bacterial communities that account for no less than 1% of the entire microbial community [33], thus masking the secondary status of bacteria. Therefore, it is difficult to detect AOB with a content below 1% by using bacterial universal primers for F357-GC/R518. For AOB, the nested PCR method is used. Firstly, by using specific primers CTO189fA/B/C and CTO654r with better binding affinity to AOB, the DNA fragments of AOB with lower content in the bacterial community can be effectively amplified, and then PCR-DGGE detection can be performed, resulting in more AOB bands in Fig. 5b) than in Fig. 5a). Secondly, due to the use of two rounds of amplification in nested PCR. Although the specificity of PCR amplification can be guaranteed, the probability of cross-contamination during the second PCR amplification will increase, which may cause some false-positive results. This is also the reason for the increase in the number of AOB bands in Fig. 5b).

Conclusions

(1) After 20 min of 60ºC thermal shock treatment, the embedded particles could achieve stable nitrification under continuous-flow conditions, and the accumulation rate of NO_2^--N reached over 90%.

(2) The PCR-DGGE technology was used to study the community structure and dynamic changes in the pre-domestication, post-domestication, and post-heat-shock stages of embedded bacterial particles. It was found that before domestication, the greatest diversity of activated sludge was observed. As domestication progressed, the total bacterial diversity decreased, the types of AOB and NOB significantly increased, and the nitrification performance of the sludge was enhanced. Thermal shock had little effect on AOB population diversity but had a significant impact on NOB. Almost all dominant NOB bacterial genera were inactivated. This provides a theoretical basis for a new type of encapsulation short-range nitrification process based on thermal shock.

(3) Some of the dominant strains of total bacteria were analyzed by cut-and-recovery clonal sequencing and phylogenetic tree analysis, and the dominant strains included β-Proteobacteria, γ-Proteobacteria, α-Proteobacteria, Nitrospira, and Uncultured. Four of the bacteria belonged to the AOB group, and one bacterium belonged to the NOB group.

(4) This study validates the core principle under a simplified hydraulic model. In practical engineering scenarios, the synergistic regulation of hydraulic conditions with physicochemical factors such as thermal shock will be key to determining process stability and efficiency, which also represents an important direction for our subsequent research.

Acknowledgments

The research work was supported by the Graduate Student Innovation Fund of North China University of Science and Technology (Grant No. 2025B09), and the Central Guiding Local Technology Development Funds Project of Hebei Province, China (Grant No. 246Z7610G, 246Z4201G).

Conflict of Interest

The authors declare no conflict of interest.

References

1. RAN X., WANG T., ZHOU M., LI Z., WANG H., TSYBEKMITOVA G. T., GUO J., WANG Y. A Novel Perspective on the Instability of Mainstream Partial Nitrification: The Niche Differentiation of Nitrifying Guilds. Environmental Science & Technology, **59** (18), 8922, **2025**.
2. KANG D., ZHAO X., WANG N., SUO Y., YUAN J., PENG Y. Redirecting carbon to recover VFA to facilitate biological short-cut nitrogen removal in wastewater treatment: a critical review. Water Research, **238**, 120015, **2023**.
3. LI Y., GENG B., GAO Y., MA Y. Effect of influent volumetric loading rates on short-cut nitrification and denitrifying phosphorus removal in anaerobic baffle reactor-membrane bioreactor system: Long term performance and microbial mechanism. Journal of Water Process Engineering, **69**, 106740, **2025**.
4. CHANG B.-Z., ZHANG S., CHEN D.-Z., GAO K.-T., YANG G.-F. Performance, kinetic characteristics and bacterial community of short-cut nitrification and denitrification system at different ferrous ion conditions. Biodegradation. **35** (5), 621, **2024**.
5. LI DONG M.Z., LI M., WANG Q., HU L. Partial nitrification start-up study running alternately between sequential batch and continuous flow. China Environmental Science, **43** (7), 59, **2023**.
6. SU Z., LIU T., GUO J., ZHENG M. Nitrite oxidation in wastewater treatment: microbial adaptation and suppression challenges. Environmental Science & Technology, **57** (34), 12557, **2023**.
7. ZHANG C., ZHANG M., CHEN W., CHEN H., WU J. NOB suppression by organic pollutants in mainstream single-stage partial nitrification/anammox (PN/A) process: Experimental evidence and modelling investigation. Chemical Engineering Journal, **498**, 155459, **2024**.
8. LIU C., WANG Y., CHEN G., YU D., ZHANG X., WANG X., TANG Z., XU A. A novel stable nitritation process: Treating sludge by alternating free nitrous acid/heat shock. Bioresource Technology, **347**, 126753, **2022**.
9. AFROZE N., KIM M., CHOWDHURY M.M., HAROUN B., ANDALIB M., UMBLE A., NAKHLA G. Effect of thermal shock and sustained heat treatment on mainstream partial nitrification and microbial community in sequencing batch reactors. Environmental Science and Pollution Research, **31** (4), 6258, **2024**.
10. ISAKA K., SUMINO T., TSUNEDA S. Novel nitritation process using heat-shocked nitrifying bacteria entrapped in gel carriers. Process Biochemistry, **43** (3), 265, **2008**.
11. YU L., LI R., MO P., FANG Y., LI Z., PENG D. Stable partial nitrification at low temperature via selective inactivation of enzymes by intermittent thermal treatment of thickened sludge. Chemical Engineering Journal, **418**, 129471, **2021**.
12. LI D., ZHONG-XIN M., LI M.-R., WANG Q.-Y., LI-JUN H. Achieving stable partial nitrification by combining heat-shock sludge and intermittent gradient aeration. China Environmental Science, **44** (7), 3719, **2024**.
13. LIU Z., CHEN Y., XU Z., LEI J., LIAN H., ZHANG J., WANG Z. Surface modification of polyurethane sponge with zeolite and zero-valent iron promotes short-cut nitrification. Polymers, **16** (11), 1506, **2024**.
14. AHMED M.E., KHAJAH M., ABDULLAH H., AL-YASEEN R. Treatment of Industrial Wastewater of Variable Quality Using Ultrasound Irradiation. Civil Engineering Journal, **11** (4), 1476, **2025**.
15. JIA M., MIAOJIE M., JING L., ZHENG S., YALEI Z. Review of Research Progress on Microbial Immobilization Technology in Wastewater Treatment. Journal of Fujian Normal University (Natural Science Edition), **38** (1), 117, **2022**.
16. LIN X., LI B., TIAN M., LI X., WANG J. Denitrification effect and strengthening mechanism of SAD/A system at low temperature by gel-immobilization technology. Science of The Total Environment, **900**, 165599, **2023**.
17. JIANG Z., ZHENG Z., WU J., LIU X., YU H., SHEN J. Synthesis, characterization and performance of microorganism-embedded biocomposites of LDH-modified PVA/SA hydrogel beads for enhanced biological nitrogen removal process. Process Biochemistry, **121**, 542, **2022**.
18. JIA-QIANG S., JUN L., GUANG-HUI C., ZHEN-JIA Z. Denitrification Using Embedded Immobilized Denitrifying Bacteria. China Water & Wastewater, **34** (23), 105, **2018**.
19. XIANG L., ZHENG-WEI P., LIAN-GANG H., PENG T., TIAN-HAO S., JUN L., ZHAO-MING Z. Optimization of nitrogen removal performance of partial nitrification AO process based on PVA-SA immobilized particles. China Environmental Science **44**, (9), 4883, **2024**.
20. NINGXIN L. Research on Application of Modified Embedded Particles in Short-Range Nitrification. Liaoning Chemical Industry, **54** (5), 715, **2025**.
21. SUN Q., KAMARUDDIN M., HUANG K., CAO Y., YUSOFF M., CHENG Y. Study on Preparation of Nano Humic Acid and Adsorption Effect of Heavy Metals in Soil. Emerging Science Journal, **9**, 2350, **2025**.
22. MUKHEEF R.A., HASSAN W.H., ALQUZWEENI S. Artificial recharge of an unconfined aquifer using treated wastewater as a climate change mitigation strategy. Civil Engineering Journal, **10**, 319, **2025**.
23. LI Z. Cells proliferation Submitted and to decay nitrification. Shanghai: Doctoral Dissertation of Shanghai Jiao Tong University. **2012**.
24. OSHIKI M., NETSU H., KURODA K., NARIHIRO T., FUJII N., KINDAICHI T., SUZUKI Y., WATARI T., HATAMOTO M., YAMAGUCHI T. Growth of nitrite-oxidizing Nitrospira and ammonia-oxidizing Nitrosomonas in marine recirculating trickling biofilter reactors. Environmental microbiology, **24** (8), 3735, **2022**.
25. HU M., ZHANG H., TIAN Y. Achieving nitrogen removal with low material and energy consumption through partial nitrification coupled with short-cut sulfur autotrophic

denitrification in a single-stage SBR. Bioresource Technology, **380**, 128999, **2023**.
26. KWON S., MOON E., KIM T.-S., HONG S., PARK H.-D. Pyrosequencing demonstrated complex microbial communities in a membrane filtration system for a drinking water treatment plant. Microbes and Environments, **26** (2), 149, **2011**.
27. CAO Q., CHEN Y., LI X., LI C., LI X. Low C/N promotes stable partial nitrification by enhancing the cooperation of functional microorganisms in treating high-strength ammonium landfill leachate. Journal of Environmental Management, **329**, 116972, **2023**.
28. CHOLET F., AGOGUÉ H., IJAZ U.Z., LACHAUSSÉE N., PINEAU P., SMITH C.J. Low-abundant but highly transcriptionally active uncharacterised Nitrosomonas drive ammonia-oxidation in the Brouage mudflat, France. Science of the Total Environment, **946**, 174312, **2024**.
29. JIAO C., QIN H., SHUXIN L., FANGYING L., SIYU Y., WEN H., YIXIN L. Nitrosation/Anaerobic Ammonia Oxidation of CRI Systems: Start-up, Regulation/Control and Performance. Environmental Science & Technology, TOMAZETTO G., OLIVEIRA V.M. Investigation of the FeFe-hydrogenase gene diversity combined with phylogenetic microbial community analysis of an anaerobic domestic sewage sludge. World Journal of Microbiology and Biotechnology, **29** (11), 2003, **2013**.
30. ZIQIAN G., WENTING D., CHAO L., JIE T., KUN D., JIANXIONG Z., FANG Z. Enhanced methanogenesis of waste activated sludge fermentation by dosing an alginate-degrading consortium. Environmental Engineering, **16** (1), 245, **2022**.
31. MUYZER G., DE WAAL E.C., UITTERLINDEN A. Profiling of complex microbial populations by denaturing gradient gel electrophoresis analysis of polymerase chain reaction-amplified genes coding for 16S rRNA. Applied and Environmental Microbiology, **59** (3), 695, **1993**.
32. JUN-XIAO M., MING-JIE J., JIAN K. Overview of Limitation and Improving Methods of PCR-DGGE in Microbial Diversity Study. Food Science, **29** (5), 493, **2008**.